JMEPEG (2012) 21:358–365
DOI: 10.1007/s11665-011-9901-8

1059-9495/$19.00

Investigation of Properties of Powder Injection-Molded Steatites

L. Urtekin, I. Uslan, and B. Tuc

(Submitted August 4, 2010; in revised form January 17, 2011)

In this study, the mechanical and micro-structural properties of injection-molded steatites were investigated experimentally. Initially, steatite powders and binders of polyethylene glycol (PEG), polypropylene (PP), and stearic aside (SA) were mixed to prepare the feedstock. The mixing powders were granulated using the extruder. The short granules in cylindrical shapes were used as the feedstock in the injection-molding operations. Solvent- and thermal-debinding processes were applied to the green samples after the molding. The samples were sintered at 1300 °C for 4 h, and a theoretical density of 98-99% was achieved. Three-point bending and tensile tests were performed on the samples which were sintered at 1200-1300 °C. The maximum three-point bending and tensile strength values were found as 154 and 47 MPa, respectively. The morphology of fractured surface was done by scanning electron microscopy whereas porosity investigations were carried out using the same microscopy. Grain growth and structure on the specimens were also investigated using transmission electron microscopy.

Keywords CIM, mechanical properties, porosity, steatite

1. Introduction

Powder-injection molding (PIM) is a method used in the production of inorganic powder engineering components. This method is improved using injection-molding equipments and debinding processes. Temperature control is highly important to achieve successful debinding. Higher solvent temperature causes swelling or cracking of the PIM component. After debinding, molded part is subjected to a sintering step, which densifies the part to give the required mechanical properties. If the used powder is ceramic, then this method is named ceramic injection molding (CIM) (Ref 1). The inability to control the processing flaws is considered by many to be the main reason for reduced mechanical performance in CIM (Ref 2, 3). An application area of this method is especially to form of low- and high-temperature ceramics (Ref 4). Nowadays, PIM production method has accepted as close tolerance and full shape production method (Ref 5). Recently, PIM has been used in micro processing such as 400 nm alumina grains and 5-μm parts in size (Ref 6). Global PIM sales exceeded the $1 billion mark (Ref 7) and is estimated that PIM market will be 2 billion dollars in 2010 (Ref 8).

Steatite ($Mg(Si_4O_{10})(OH)_2$) is a natural mineral. It has very good mechanical and electrical properties. Steatite porcelains are very good applications in electrical and electronic industry by showing low power loss coefficient, low moisture, absorption and good impact receptivity. After sintering, steatite can be soft and has good thermal shock receptivity.

Steatite has applications such as socket, control units, insulating bed, low voltage power protection, high temperature resistance and plates. Thin sheet heater is one of the application areas of porous steatite. Other applications include heating element holders, stand off insulators, interlocking insulating beads, split bush insulators, lamp bases and caps, regulator parts (Ref 9). Karatas et al. worked on rheology of prepared feedstock produced by steatite powder and polyethylene-based binders. PE-based binder formulation has shown good homogeneity, high stability, a low viscosity at a processing temperature, a high flow behavior index (Ref 10). Karatas et al. also determined the adequate temperature and pressure for PIM produced feedstocks manufactured with polyethylene glycol (PEG)-based binders, steatite and 316L stainless steel. PEG-based binder systems have shown very good rheological properties for injection moulding with steatite powder and 316L stainless steel powder (Ref 11). Mielcarek et al. prepared 90 wt.% talc and 10 wt.% barium carbonate by mixing in ball milling for 24 h and adding 10 wt.% binder after mixing. These feedstocks were wet pressed at 100 MPa pressure and sintered at 1380 °C. It was found that the stabilization of protoenstatite in steatite body is achievable by the development of small crystals (Ref 12). Yang and Cheng researched the effects of sintering temperature on density by adding B_2O_3 to MCAS ($MgO-CaO-Al_2O_3-SiO_2$) (Ref 13).

2. Experimental Procedure

The steatite powder was supplied by Kale Chemistry Co., Turkey. The chemical composition of the experimental powder (in mass percent) is 60% SiO_2, 30% MgO, 2.5% Al_2O_3, 1.0% CaO%, 1.5% Fe_2O_3, 0.5% (Na_2O_3 + K_2O), and 4.5% tempering losses. Density of the powder was 2.7 g/cm^3. Powder size is analyzed using Malvern Mastersizer E laser particle sizer. Mean

L. Urtekin, Department of Mechanical Engineering, Dumlupinar University, Kutahya, Turkey; and **I. Uslan** and **B. Tuc**, Department of Mechanical Engineering, Gazi University, Maltepe, Ankara, Turkey. Contact e-mails: lurtekin@dpu.edu.tr, iuslan@gazi.edu.tr, and btunc@gazi.edu.tr.

particle size of as-received sample was measured as 15.12 μm. It was reduced to 3.96 μm by milling for 2 h (Fig. 1). Milling was carried out by using zirconia balls of 10-mm diameter and ball-to-powder ratio of 3:1.

The organic binder system was a mixture of PEG (polyethylene glycol), PP (propylene), and SA (stearic acid) with PEG:PP:aSA ratio of 65:30:5 by weight in dry atmosphere. The binder was mixed the steatite powder by 50-60% in vol. Maximum powder and minimum binder amount, feedstock flow type, and injection-molding temperature were determined by trying different powder and binder ratios. The full plasticized feedstock was tested in the capillary rheometer to measure the suspension viscosity at a temperature range of 170-200 °C. The extruded pellets used in the rheology had cylindrical shape with 3 mm in diameter and 2-4 mm in length. The relationship between shear rate and viscosity was used as a reference for the subsequent molding process. The pellets were injection molded using Arburg Allrounder 220S and green bending and tensile samples were produced. The injection parameters were given in Table 1. Figure 2 shows the specimen's dimension of molded tensile and bending part.

Solvent extraction and thermal decomposition methods were applied to the specimens to remove the binder system after the molding. The molded green samples were immersed in water, which was used as a solvent to remove almost all of the binder in the molded green part at 60 °C for 24 h, excluding PP and SA. During the sintering process, PP and SA were debound by thermal method. The heating rate was 1 °C/min up to 400 °C in the thermal-debinding processes. The samples were held 30 min at 400 °C. Thereafter, the samples were heated to 550 °C by 1 °C/min and held for 60 min at this temperature. After finishing pre-sintering or binder burn out, the sintering was carried out at 1200-1300 °C. The heating rate for the sintering temperature was 5 °C/min—the holding time was 2-4 h at this temperature, and sintering atmosphere was air. The cooling rate from the sintering temperature was 5 °C/min. Densities of the sintered samples were calculated based on Archimedes' principle. All the specimens' surfaces were coated with a thin film by dipping into the solution of 5 wt.% paraffin wax in 95 wt.% xylene. Linear shrinkage values were calculated by measuring the dimensions before and after the sintering processes.

Mechanical properties of the sintered specimens were obtained by tensile and three-point bending tests. Tensile and bending tests were performed using Schimadzu tensile testing machine of 5 kN capacity at Gazi University.

Microstructure examinations were carried out using JEOL JSM-6300 LV scanning electron microscopy (SEM) and Olympus optic microscopy at Gazi University. Chemical analysis was performed using the energy disperse spectrometer (EDS) of SEM at Gazi University. The crystal phases of the sintered steatite specimens were determined using Ringaku x-ray diffractometer (XRD) at Dumlupinar University. Transmission electron microscopy (TEM) was carried out using JEOL 2100 HRTEM at TUBITAK-MAM. The samples were cut into approximately 3 mm^2 pellets and mounted on a copper ring for better grounding to avoid charging of the samples during TEM operation for measurements. Then, the samples were ground using polisher down first to 100 μm, dimpled with a Cu wheel and 6-, 3-, and 1-μm diamond paste, and then down to 5 μm and argon ion sputtered to electron transparency at an angle of 8° and ion energy of 4 keV (Ref 9).

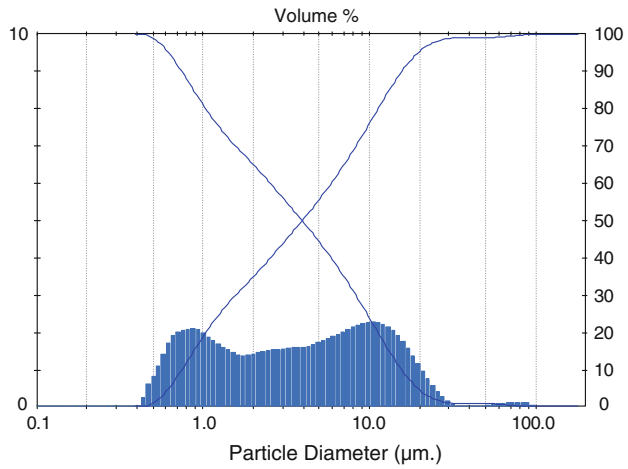

Fig. 1 Particle size distribution of the steatite powder after the milling for 2 h

3. Result and Discussion

The properties of the green, the brown, and the sintered specimens are shown in Table 2. The green specimens consist of steatite and binder system just after the molding, whereas the brown specimens consist of nearly steatite powder after the solvent debinding. Amounts of PEG debound in water were 90.7 and 92.2% for the bending and the tensile samples, respectively. The green densities of the bending and the tensile samples were also 70 and 72%, respectively. Increasing of the optimum sintering temperature was ensured the maximum density. The maximum theoretical density was calculated 99% after the sintering process at 1300 °C.

Variation of the volumetric shrinkage with the temperature is shown in Fig. 3. Sintering shrinkage has been found uniform and isotropic and no distortion can be observed after sintering process. Volumetric shrinkage ratio was found close to the value of the sample with addition of 42% PEG/PP/SA binder mixture. The values for bending and tensile samples were 41.96 and 41.9%, respectively.

The variation of the mechanical properties with the temperature is shown in Fig. 4. The bending strength of steatite is given as 124-140 MPa in the literature (Ref 14). The maximum bending strength of the steatite was obtained as 154 MPa under the sintering conditions of 1300 °C and 4 h. These sintering conditions also gave maximum tensile strength of 47 MPa.

Figure 5 shows the relationship the porosity versus bending and tensile strengths. As seen from the Fig. 4, the less porosity, the greater the strength values. The curves in Fig. 5 show that this relationship was determined with a correlation analysis. The present experimental data are consistent with the equations below:

$$\sigma_b = 142.9\ \exp(-13,92\eta) \quad \text{for bending strength}$$

$$\sigma_t = 44.32\exp(-17,81\eta) \quad \text{for tensile strength}$$

where η is the porosity, σ_0 is the ultimate tensile strength, $\sigma_{b,t}$ are the bending and tensile strengths.

The SEM micrographs of steatite specimens' fractured surface provided in Fig. 6 and 7 reveal clearly different fracture mechanisms between the stages of sintering process. The fractured surface for the samples of the lowest tensile strength had a wide and deep crack (Fig. 6a). When the tensile strength

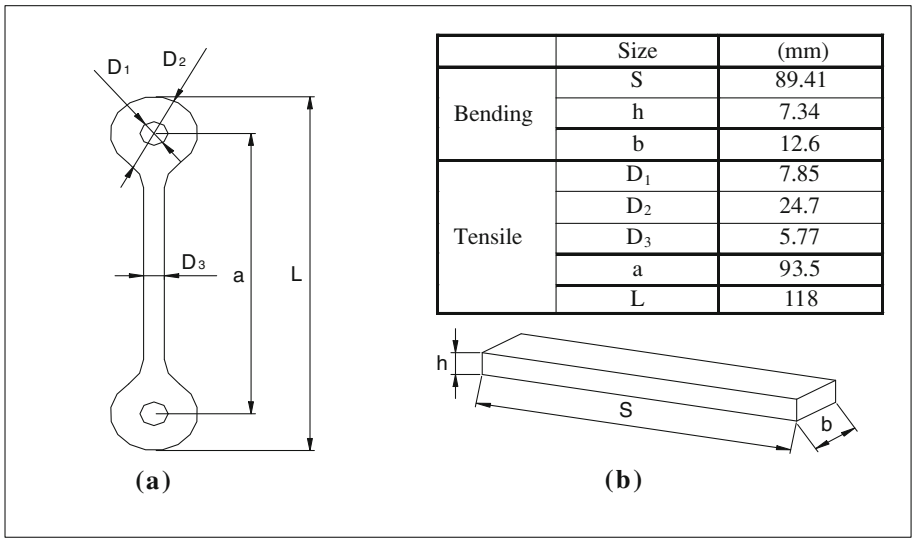

	Size	(mm)
Bending	S	89.41
	h	7.34
	b	12.6
Tensile	D_1	7.85
	D_2	24.7
	D_3	5.77
	a	93.5
	L	118

Fig. 2 Sizes of the green tensile (a) and bending specimens (b)

Table 1 PIM operation parameters

	Molding pressure, bar	Holding pressure, bar	Barrel temperature, °C	Feedstock flow rate, cm^3/s	Mold temperature, °C
Bending sample	1000-1250	600	35-185-190-195-200	15	20
Tensile sample	1350	600	35-190-195-200-205	17-25	20

Table 2 The properties of injection-molded, solvent debound and sintered samples

Tests	Properties	Green sample	Brown sample	Sintered sample
Bending	Weight, g	16.251	14.095	12.590
	Height, mm	89.41	…	73.15
	Width, mm	7.34	…	6.05
	Thickness, mm	12.58	…	10.31
	Removing PEG 8000, %	…	90.7	…
	Dimensional shrinkage, %	…	…	18.18
Tensile	Weight, g	13.594	11.762	10.535
	Height, mm	118	…	96.56
	∅ diameter, mm	5.77	…	4.69
	Removing PEG 8000, %	…	92.2	…
	Dimensional shrinkage, %	…	…	18.17

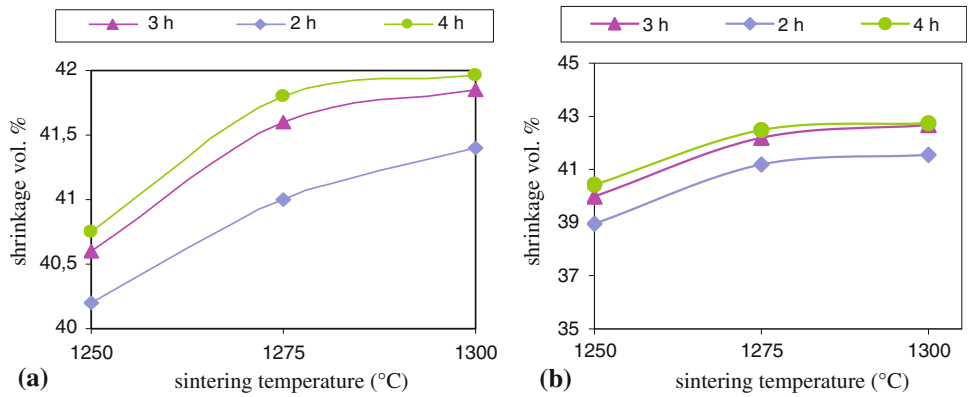

Fig. 3 Volumetric shrinkage of bending samples (a) and tensile samples (b)

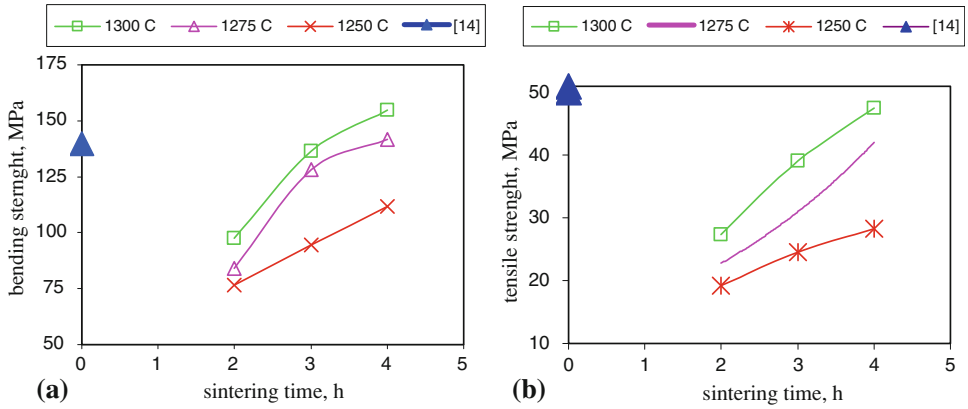

Fig. 4 (a) Bending and (b) tensile strength versus sintering temperature

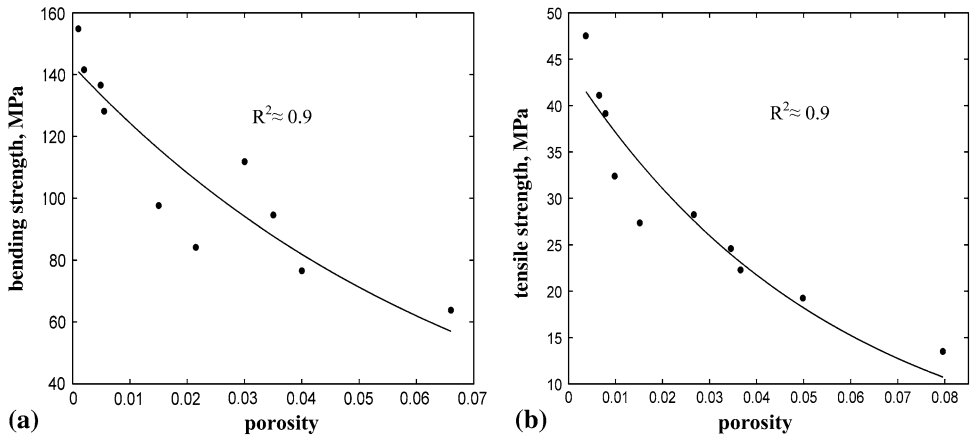

Fig. 5 Porosity versus strength of bending (a) and tensile (b)

increased, fracture surface had more or less homogenous porosity (Fig. 6b-d). Same case is observed for bending tests as well (Fig. 7).

Images obtained by SEM analyses are illustrated in Fig. 8. Sintering process was carried out for different temperatures between 1200-1300 °C and holding time 4 h (Fig. 8). Sintered samples have open porosity at 1200 °C (Fig. 8a). The porosities got smaller when sintering temperature was increased up to 1250 °C (Fig. 8b). Once sintering temperature reached 1275 °C, porosities were spherical and wholly isolated (Fig. 8c). If sintering temperature was increased to 1300 °C, most of porosities were close and the samples were near full density (Fig. 8d). Densities of the sintered samples were measured using Archimedes' principle. All the sample surfaces were coated with a thin film by dipping into the solution of 5 wt.% paraffin wax in 95 wt.% xylene. For 1300 °C for 4 h, maximum linear shrinkages of tensile and bending samples were 18.17 and 18.18%, respectively.

The specimen sintered at 1200 °C corresponds to the adhesion stage of sintering, 1250 °C is the intermediate stage, and those at 1275 and 1300 °C correspond to the final stage (Fig. 8). The density increases in the final stage, when the pores become spheroidal and shrink, which are no longer connected to the compact surface. These pores are termed closed pores (Ref 9).

XRD pattern of the molded steatite specimens sintered at 1300 °C for 4 h. XRD patterns in Fig. 9 showed that relative peak intensity of proto-enstatite crystals was stably increased. Lower and regularly distributed pores in CIM parts lead to improvement in mechanical properties which are better than those in the case of classical parts. This was supported by the strength tests. However, if protoenstatite crystals are not properly stabilized, then transformation to the polymorph, clinoenstatite at room temperature will occur, and this martensitic type of transformation implies a volume change that leads to an extensive material cracking. For many years, this has been the origin of material damage during manufacturing and service (Ref 15).

EDS scanning and elemental analysis were applied on the SEM microstructure with a 1000 magnification (Fig. 10). Table 3 shows EDS analysis results by giving elements' weight and atomic ratios.

The TEM analysis results are given Fig. 11. Figure 11(a) shows grain size and structure of the samples sintered at 1300 °C for 99% theoretical density. Grain size was found to be nearly 1 μm. Without seeing porosity on these structures, suggested structure was very dense. Figure 11(b) shows ⟨101⟩ zone axis diffraction pattern. Figure 11(c) show diffraction pattern for ⟨110⟩ zone patterns. These patterns were consonant with the patterns of the protoenstatite.

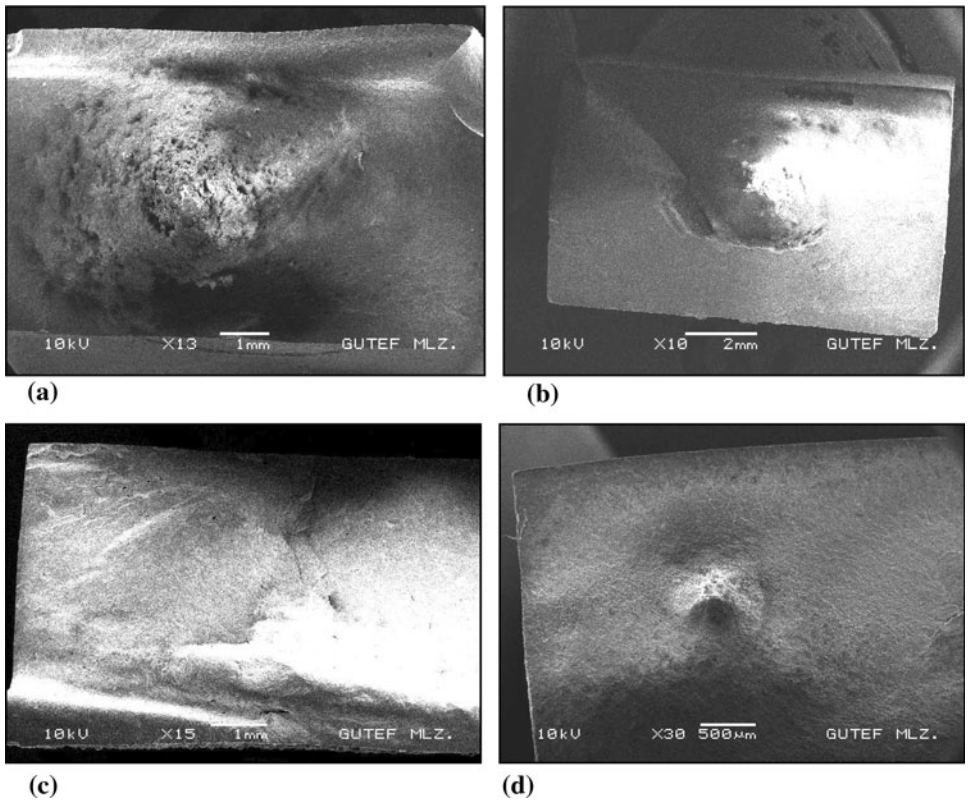

Fig. 6 Fractured surfaces of the bending specimens which have minimum and maximum strengths. (a) Theoretical density 90%, σ_b = 63.9 MPa, (b) theoretical density 93%, σ_b = 76.6 MPa, (c) theoretical density 98%, σ_b = 136.6 MPa, and (d) theoretical density 99%, σ_b = 154.8 MPa

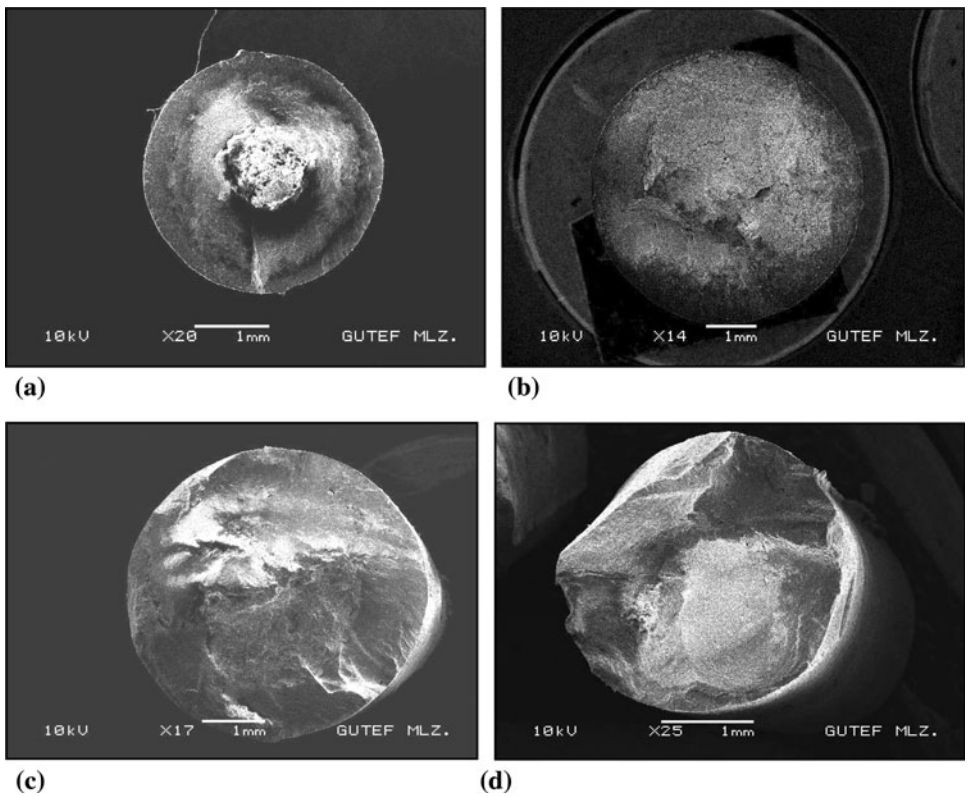

Fig. 7 Fractured surfaces of the tensile specimens which have minimum and maximum strengths. (a) Theoretical density 90%, σ_t = 13.5 MPa, (b) theoretical density 94%, σ_t = 24.6 MPa, (c) theoretical density 96%, σ_t = 32.4 MPa, and (d) theoretical density 99%, σ_t = 47.52 MPa

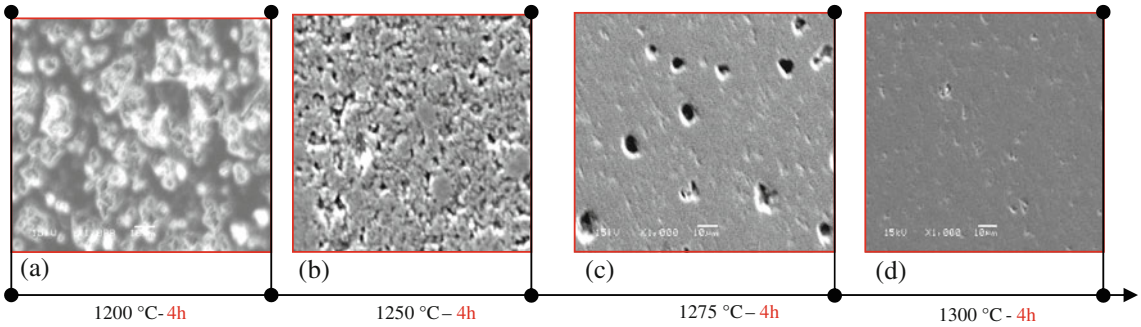

Fig. 8 Pore structures in sintered samples (SEM images). (a) open porosity, (b) surface contact, (c) isolated porosity, and (d) exactly density

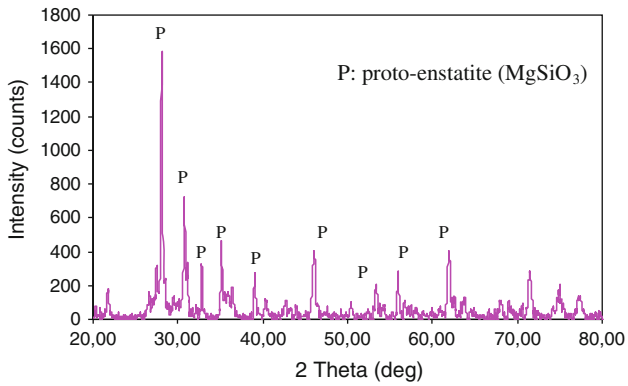

Fig. 9 XRD patterns of injection-molded steatite as a function of solid content sintered at 1300 °C for 4 h

4. Conclusions

1. Tensile and bending specimens of steatite have been successfully fabricated without any distortion through the CIM.
2. Theoretical density of the specimens has been controlled from 90 to 99 by varying the sintering temperature ranging from 1200-1300 °C.
3. The pores of sintered specimens appeared to become more rounded and isolated in their distribution as the sintering temperature increased. The closure of pores enhanced strength of sintering specimen.
4. The tensile and bending strength tests showed an increase with the increasing sintering temperature. The steatite obtained by CIM shows a good strength. The maximum strengths of bending and tensile test values were found 154 and 47 MPa, respectively.

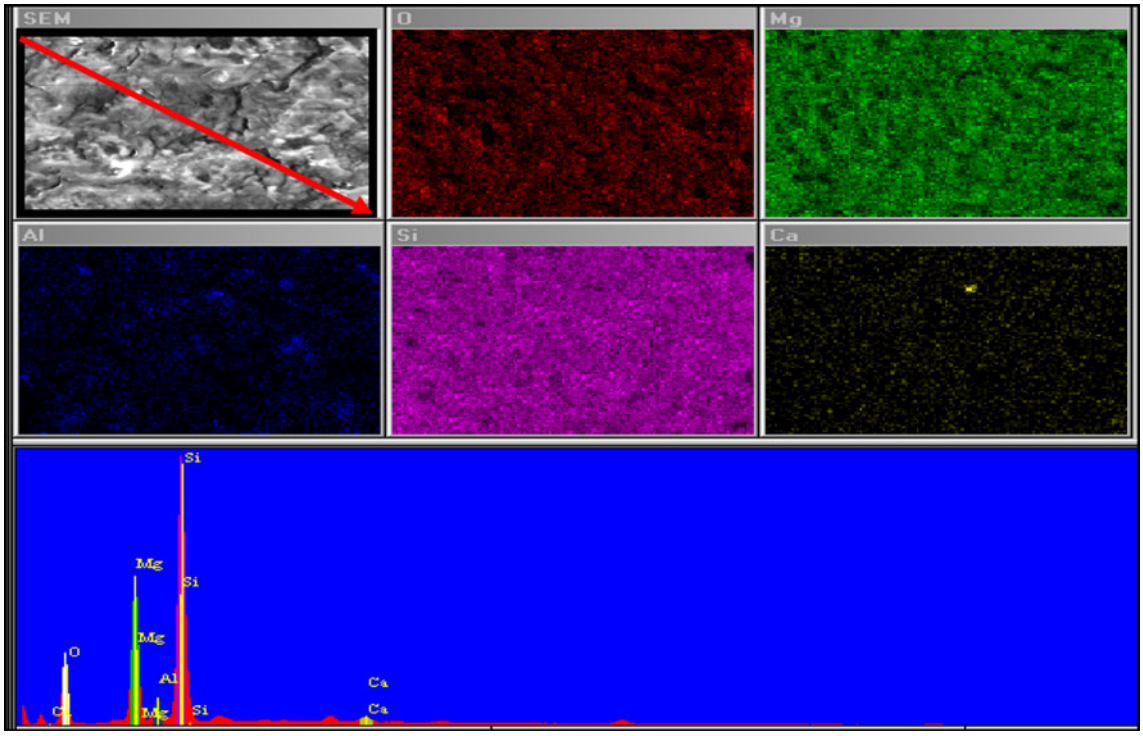

Fig. 10 Measuring the energy disperse spectrometer (EDS) of steatite sintered at 1300 °C for 4 h

Table 3 Chemical analysis of the samples in EDS

Analyses	O	Mg	Al	Si	K
wt.%	45.55	20.93	2.88	30.00	0.64
at.%	58.11	17.57	2.18	21.80	0.33

5. The temperature 1300 °C was an optimum finding for formation of small, well-crystallized, protoenstatite crystals.
6. As a result of TEM analysis, the distribution of atoms was found to show protoenstatite structure. The grain size was found to be nearly 1 μm.

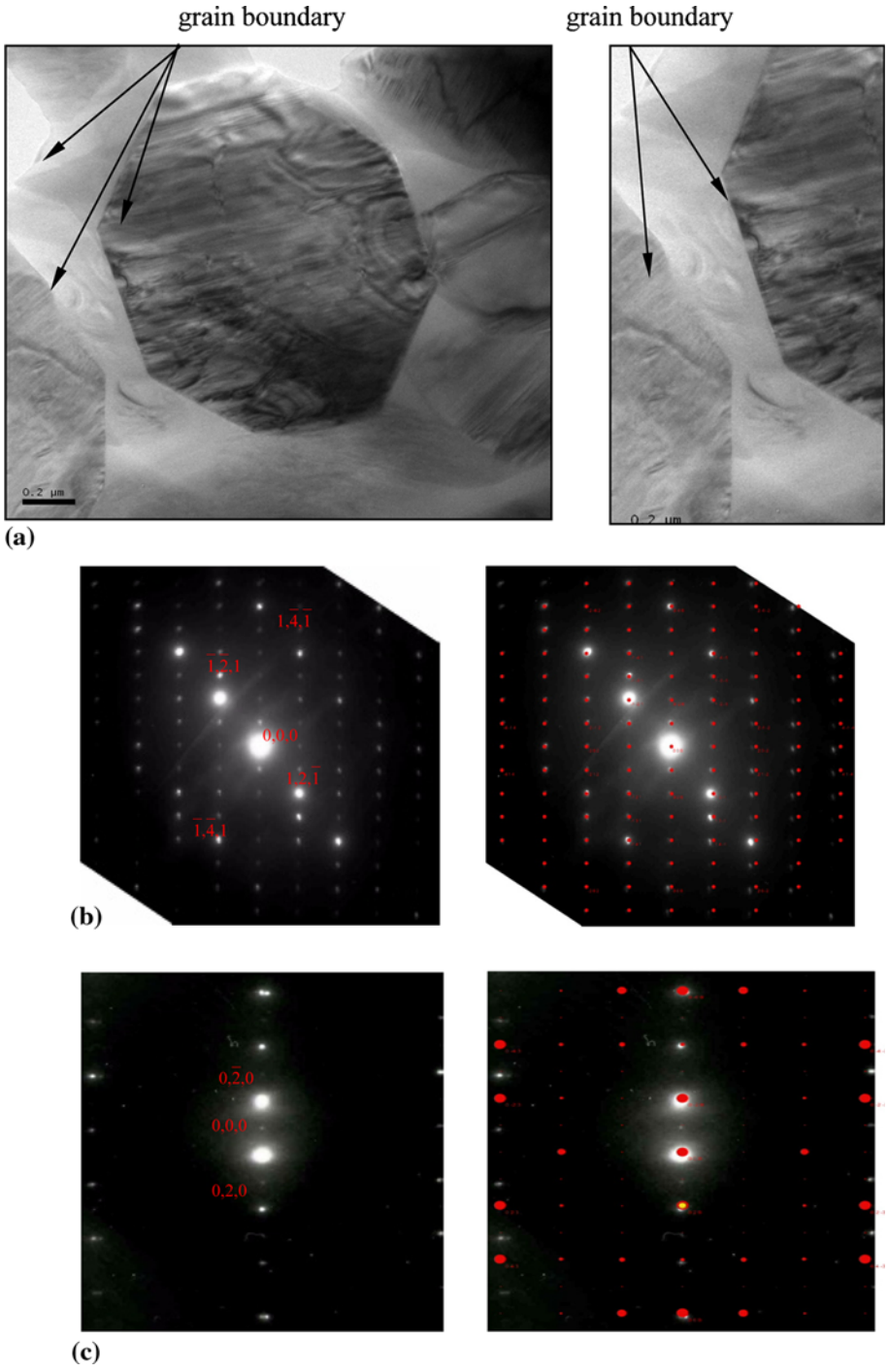

Fig. 11 TEM micrograph of the steatite (a), ⟨101⟩ zone axis diffraction pattern (b), and ⟨110⟩ zone axis diffraction pattern (c)

Acknowledgments

The authors are grateful to Prof. Dr. Suleyman Saritas. The authors acknowledge the support of Gazi University (DPT Projects Nos. 2001K120590 and 2003K120470) labs for facilitating the experimental studies.

References

1. R.M. German, *Powder Metallurgy and Particulate Materials Processing*, Metal Powder Industries Federation, Princeton, NJ, 2005
2. M.J. Edirisingle and J.R.G. Evans, Review: Fabrication of Engineering Ceramics by Injection Moulding. II. Tecnigues, *Int. J. High Temp. Ceram.*, 1986, **2**, p 249–278
3. R.M. German, *Powder Injection Molding*, Metal Powder Industries Federation, Princeton, NJ, 1990
4. C. Karatas, "Rheology for Feedstocks Used Powder Injection Moulding," Ph.D. thesis, Gazi University, Ankara, 1997
5. R.M. German and A. Bose, *Injection Molding of Metals and Ceramics*, Metal Powder Industries Federation, Princeton, NJ, 1997
6. R. Zauner, Micro Powder Injection Moulding, *Microelectron. Eng.*, 2006, **83**, p 1442–1444
7. R.M. German, PIM Breaks the $1 bn Barrier, *Met. Powder Rep.*, 2008, **63**(3), p 8–10
8. C. Karatas and S. Sarıtas, Powder Injection Molding: A High Technology Manufacturing Process, *J. Fac. Eng. Archit. Gazi Univ.*, 1998, **13**(2), p 193
9. L. Urtekin, "Investigation of the Effect of Molding and Sintering Parameters on Properties of Powder Injection Molded Steatite Ceramics," Ph.D. thesis, Gazi University, Ankara, 2008
10. C. Karatas, A. Kocer, H.I. Unal, and S. Sarıtas, Rheological Properties of Feedstocks Prepared with Steatite Powder and Polyethylene-Based Thermoplastic Binders, *J. Mater. Process. Technol.*, 2004, **152**, p 77–83
11. C. Karatas, M. Gokten, H.I. Unal, S. Sarıtas, and I. Uslan, Investigation of Reological Properties of the Feedstocks Composed of Steatite and 316L Stainless Steel Powder and PEG Based Resins, *Euro PM*, 2005, p 367–373
12. W. Mielcarek, D.N. Wozny, and K. Prociow, Correlation Between $MgSiO_3$ Phases and Mechanical Durability of Steatite Ceramics, *J. Eur. Ceram. Soc.*, 2004, **24**, p 3817–3821
13. C.F. Yang and C.M. Cheng, The Influence of B_2O_3 on the Sintering of MgO-CaO-Al_2O_3-SiO_2 Composite Glass Powder, *Ceram. Int.*, 1999, **25**(4), p 383–387
14. Vogt Ceramic Component "Material properties", 2008, http://www.vogt-ceramic.de/en/mproperties.htm
15. E. Vela, M. Peiteado, F. Garcia, A.C. Cabellero, and J.F. Fernandez, Sintering Behaviour of Steatite Materials with Barium Carbonate Flux, *Ceram. Int.*, 2007, **33**, p 1325–1329